Solid state emission enhancement of 9,10-distyrylanthracene derivatives and amplified spontaneous emission from a large single crystal†

Bin Xu,[a] Honghua Fang,[b] Yujie Dong,[a] Feipeng Chen,[a] Qidai Chen,[b] Hongbo Sun[b] and Wenjing Tian*[a]

Received (in Montpellier, France) 20th April 2010, Accepted 29th June 2010
DOI: 10.1039/c0nj00300j

Methyl-substituted 9,10-distyrylanthracene was synthesized by a simple Heck reaction and its photophysical properties investigated. Tight intermolecular stacking through supramolecular interactions in the crystal not only induced strong fluorescence emission with a high fluorescence efficiency of 35% but also conducted the formation of large size and high quality needle-like single crystals. Amplified spontaneous emission (ASE) with a low threshold value of 10 μJ pulse^{-1} was observed.

Fluorescent organic materials have been extensively investigated as active gain media for optically-pumped solid-state lasers.[1] However, most fluorescent organic materials have a very high fluorescence efficiency in solution, but this generally decreases in the solid-state. This decreasing fluorescence efficiency in the solid-state is mainly attributed to high non-radiative decay rates by excitation energy trapping or low-radiative rate constants by H-type aggregation, which is a specific case of excitonic coupling.[2] Consequently, increasing attention has been paid to enhancing the solid-state fluorescence efficiency of fluorescent materials. Recently, several intriguing cases have been reported for organic fluorophores that show unique enhanced emission rather than fluorescence quenching in the solid-state.[3] Although the origins of these enhanced emissions are still in debate, it is assumed that this unique fluorescence phenomenon is related to the effects of intramolecular planarization, the formation of specific aggregation and the blockage of non-radiative relaxation pathways of the excited species.[4] Recent studies on the crystals of silole derivatives and other molecules have revealed that their common structural characteristics are a twisted conformation in the solid-state, which suggests that the emission enhancement of the crystals is caused by restricted intramolecular vibrational and rotational motions in the solid-state.[5] Thus, investigating the single crystal structure of molecules is an important way to understand and clarify the relationship between their molecular packing and emission properties in the solid-state. On the other hand, the phenomenon of amplified spontaneous emission (ASE) has been demonstrated in a broad range of conjugated polymers, oligomers and dye-doped polymer systems, though the main factors to affect the applications of those materials are their low stability and inferior carrier mobility.[6] Organic single crystals may be promising candidates for ASE applications due to their high thermal stability, good charge transport properties and remarkable optical anisotropy, induced by the crystalline assembly of molecules. Nevertheless, only a few works have reported on ASE in organic single crystals, because it is difficult to obtain large size and high quality crystals with a high photoluminescence quantum yield.[7]

Recent work in our group has demonstrated that 9,10-distyrylanthracene derivatives show high fluorescence efficiency in their crystals.[8b] Here, we report on a large size and high fluorescence efficiency crystal of methyl-substituted 9,10-distyrylanthracene (BMSA). The purpose of the structure modification is to control the molecular packing. Tight intermolecular stacking *via* supramolecular interactions in the crystal not only induces strong fluorescence emission but also conducts the formation of large size and high quality needle-like single crystals. To further demonstrate its potential applications in an organic crystal-based laser, the amplified spontaneous emission (ASE) properties of the crystals were investigated. A low threshold value of 10 μJ pulse^{-1} and a full-width at half-maximum (FWHM) of 10 nm were obtained from the large size needle-like crystals.

BMSA was synthesized by a typical *trans*-selective Heck coupling reaction.[8] BMSA shows almost no fluorescence ($\Phi_F < 1\%$) in THF solution but its crystals show strong fluorescence in the green spectral region with a Φ_F efficiency up to 35% (Φ_F in the solid-state is obtained in a calibrated integrating sphere), as shown in Fig. 1(b).

A single crystal of BMSA was prepared by vaporizing a mixture of chloroform and ethanol slowly at room temperature under the rigorous exclusion of light, and its structure was characterized by X-ray crystallography.† The crystal data reveals that the BMSA molecule lies about an inversion centre and has a *trans*-conformation in the molecule, with relatively large torsion angles of 67° between the anthracene center and the vinylene moieties substituted at the 9- and 10-positions. On the other hand, the structure of BMSA and the optimized geometry of isolated BMSA (Fig. 1(a)) demonstrates a twisted configuration of the molecule with a torsion angle of 54° in the gas phase or dilute solution due to the large internal steric hindrance between the hydrogen on the phenyl ring of the anthracene moieties and the hydrogen on the vinylene moieties.[9] The origin of the non-emission of BMSA in solution

[a] *State Key Laboratory of Supramolecular Structure and Materials, Jilin University, 2699 Qianjin Avenue, Changchun 130012, P. R. China. E-mail: wjtian@jlu.edu.cn; Fax: + 86 431 85193421; Tel: + 86 431 85166368*
[b] *State Key Laboratory on Integrated Optoelectronics, College of Electronic Science and Engineering, Jilin University, 2699 Qianjin Avenue, Changchun 130012, P. R. China*

† CCDC reference number 774731. For crystallographic data in CIF or other electronic format see DOI: 10.1039/c0nj00300j

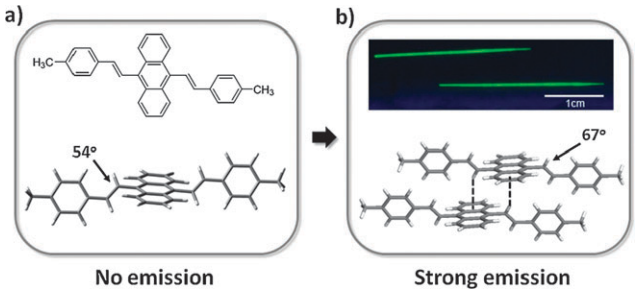

Fig. 1 (a) The molecular structure of BMSA (top) and the optimized geometry of isolated BMSA (bottom). (b) A crystal of BMSA under UV light irradiation (top) and the BMSA structure fixed by CH/π interactions in the crystal (bottom).

should be related to the twisted configuration and the corresponding intramolecular torsional motions around the double bond beside the anthracene moieties. These intramolecular motions can lead to fast non-radiative relaxation and the reduction of fluorescence efficiency in solution.[5]

From an analysis of the structure and packing arrangements of the crystal, we found that the CH/π interactions play a crucial role in the molecular packing, and they are also important in terms of the non-planar conformations of the BMSA. The unit cell of BMSA is monoclinic with a space group $P2_1/c$. Its packing arrangement is shown in Fig. 2. A CH/π hydrogen bond (interaction I) is formed between two molecules with an interaction distance of 2.79 Å and an angle of 147.9°, where the vinylene moiety along the long axis of one molecule acts as a H-donor and the corresponding phenyl ring of anthrylene moiety of the adjacent molecule acts as a H-acceptor. At the same time, another CH/π hydrogen bond (interaction II) is formed between the two molecules with an interaction distance of 2.91 Å and an angle of 166.8°, where the methyl of the phenyl ring acts as a H-donor and the corresponding anthrylene moiety of the adjacent molecule acts as a H-acceptor. In crystals of BMSA, the molecules pack into molecular columns along the *a*-axis and slide to their neighbors along the long molecular axis within one column due to interaction I. On the other hand, the molecules are packing into a zig-zag motif along a mirror glide plane in one layer due to interaction II.[10] This indicates that the supramolecular interactions in the BMSA crystal are relatively strong.[11] It is the CH/π hydrogen bonds that fix the anthrylene moieties and the peripheral double bonds, preventing free torsional motions around the double bonds. Assisted by strong supramolecular interactions, the molecule not only becomes more stable and distorted in the crystal lattice, but also tends towards tight intermolecular packing. Therefore, supramolecular interactions play an important role in the strong fluorescence of BMSA crystals.[12]

To fully understand the origin of emission enhancement, Fig. 3 presents the absorption and PL spectra of BMSA at room temperature and 77 K. Compared to the absorption spectrum of BMSA at room temperature, the absorption spectrum at 77 K clearly shows vibrational structure and a red shift, indicating a reduction in conformational disorder and a higher polarizability of the low temperature glass.[13] The PL spectrum of BMSA in THF solution at room temperature

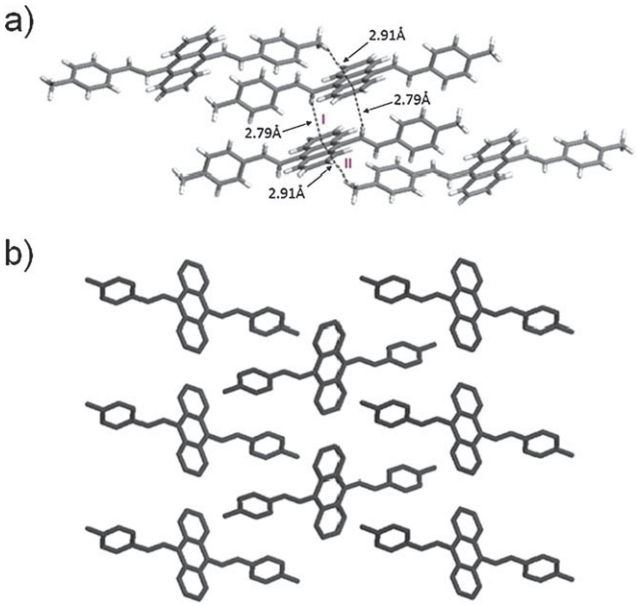

Fig. 2 (a) Intermolecular interactions I and II in crystals of BMSA. (b) A molecular packing diagram of BMSA under CH/π interactions viewed along the *a*-axis. The hydrogen atoms have been omitted for clarity.

shows a weak and board emission band. Upon cooling to 77 K, the non-emitting BMSA becomes strongly fluorescent in the glassy state, and the intensity of the PL is almost 120-fold higher than that at room temperature. Meanwhile, the emission of BMSA at 77 K shows a blue shift compared to that of a dilute solution at room temperature. This can be attributed to the enhanced potential barrier for free intramolecular torsional motion around the double bonds in such a rigid medium at low temperature and the formation of more distorted configurations resulting in a blue-shifted emission.[5,8b] Thus, the strong emission of BMSA in a glassy solvent at low temperature may have the same origin as the strong emission due to restricted intramolecular motion. Otherwise, different from the PL spectrum of the single crystal, the PL spectrum of BMSA in a low temperature solution clearly shows vibrational structure and a blue shift. This feature indicates that the emission properties at low temperature may arise from single molecules with restricted intramolecular motion caused by glassy solvent molecules, which is different from the restriction of the environment in single crystals due to supramolecular interactions.

Time-resolved measurements of BMSA in dilute THF solution and in single crystals at room temperature were performed using time-correlated single-photon counting (TCSPC) with excitation at λ_{ex} = 405 nm; typical results (λ_{fl} = 630 nm for solution and λ_{fl} = 530 nm for crystal, respectively) are shown in Fig. 4. The data points are the experimental data and the solid lines are the fitting curves based on exponential functions.[14] From Fig. 4, one can see that the fluorescence of crystals of BMSA decays very rapidly compared to that of its solutions. The BMSA solution fluorescence shows a single exponential decay with an emission lifetime of ~2.29 ns. However, for BMSA crystals, the following double-exponential function can simulate its decay

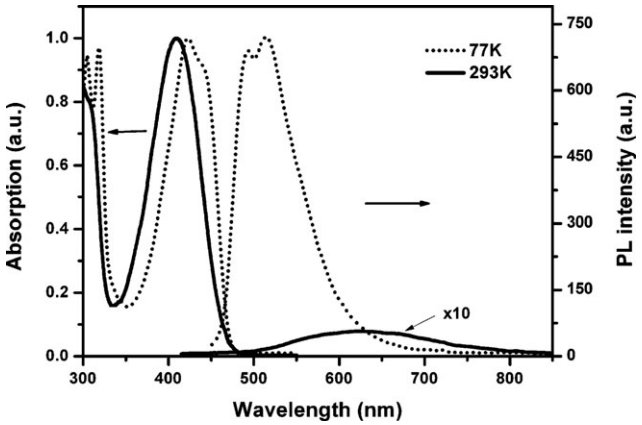

Fig. 3 Room temperature (—) and 77 K (···) absorption spectra of BMSA in methyl-THF (1×10^{-5} mol L^{-1}), and the PL spectrum of BMSA in dilute THF (1×10^{-5} mol L^{-1}). The absorption spectra are normalized.

behavior better than can the single-exponential one. This reveals that the excited states of BMSA molecules in single crystals decay through two pathways: one pathway shows a rapid decay with a decay coefficient of 0.97 and a lifetime of ~0.85 ns; the other pathway shows a slow decay character with a coefficient of 0.03 and a lifetime of ~7.21 ns. These observations indicate that the contribution of the slow decay becomes negligible and that of the rapid decay became dominant in the emission transient processes of crystals. The decrease of the lifetime in single crystals against solutions is again indicative of the role of supramolecular interactions in the emission process.

Under the strong driving force of CH/π hydrogen bonding interactions, BMSA molecules can easily form large needle-like single crystals with a length of around 3 cm and a width of several hundred microns (a photograph is shown in Fig. 1(b)), suggesting its potential application in organic solid-state lasers. To obtain an in-depth characterization of optical gain properties, ASE of a single crystal was investigated. Optical pumping was generated by the second harmonic (400 nm) of a Ti:sapphire optical amplifier with a maximum pulse energy 1.5 mJ and a pulse duration of 120 fs. The laser beam was focused by using a quartz cylindrical lens into a strip whose spot area was 5×1 mm^2 and parallel to the long axis of the crystal, which was glued to the quartz substrate. The PL emission was collected from the edge of the crystal and sent through an optical fiber to the spectrometer. All measurements were carried out at room temperature. Fig. 5 displays the PL spectra of this crystal as a function of pump laser energy, and the insert is the PL emission peak changes as a function of pump laser energy. The emission spectra (including conventional PL spectra) for the BMSA single crystal exhibit a broad feature under weak incident intensities that corresponds to spontaneous emission. As the pump intensity is increased, a sharp PL spectrum centered at 524 nm and a gradual blue-shift of the ASE peak maximum are observed, indicating that the ASE process occurs on a timescale faster than the spectral diffusion that occurs during the first few ps after photoexcitation.[1c] Fig. 6 shows the dependence of the FWHM and the integrated peak intensity of the PL spectrum as a function of excitation fluence. At a low pump fluence of 5.1 μJ $pulse^{-1}$, the FWHM of the emission spectrum was approximately 60 nm. When the pump fluence was gradually increased, the FWHM decreased to 10 nm. The relationship between the peak intensity and the pump energy was not linear, being characterized as ASE caused by stimulated emission. The threshold of ASE can be extracted from the change of slope of the pump intensity dependence, which is located at 10 μJ $pulse^{-1}$. In addition, the FWHM of the emission spectrum was dramatically reduced from 60 to 10 nm in the region of the threshold. Upon further increasing the pump energy, gain narrowing was halted and the FWHM changed no further. The main mechanism for the observed gain-narrowing is attributed to ASE by the observation of the waveguiding property and the effect of pump length on light amplification.[15]

To summarize, we have developed a new molecule, BMSA, with a solid-state emission enhancement and demonstrated that tight intermolecular stacking through supramolecular

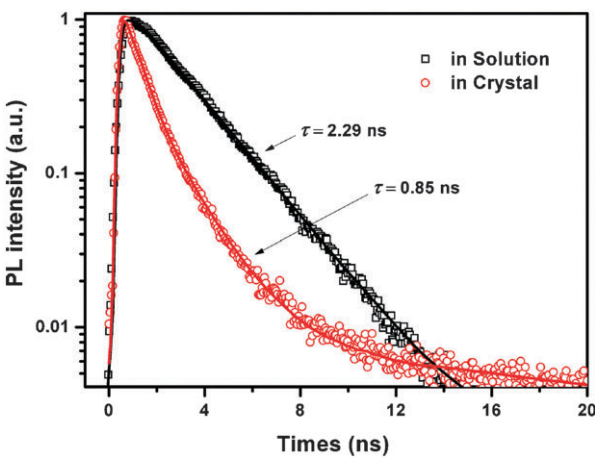

Fig. 4 Time-resolved fluorescence spectra of BMSA in THF solution (□) and single crystals (○) at room temperature measured by TCSPC. The solid lines are the fitting curves based on exponential functions.

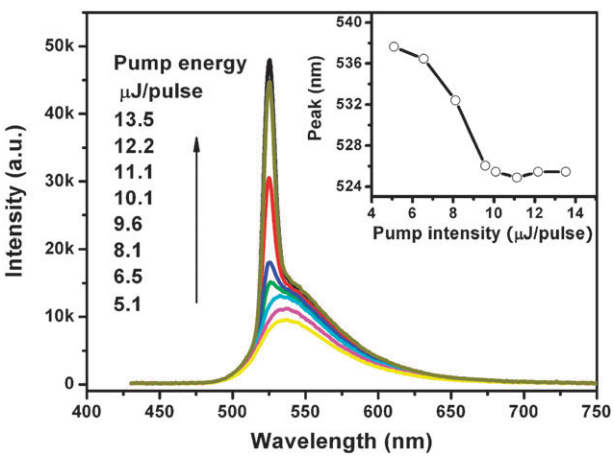

Fig. 5 The PL spectra of a BMSA single crystal as a function of pump laser energy. Inset: PL emission peak changes as a function of pump laser energy.

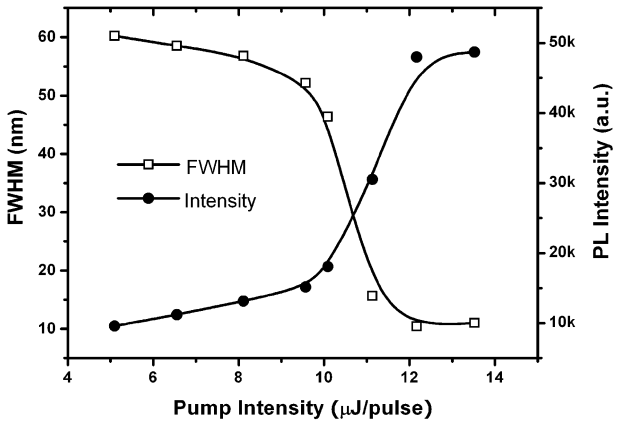

Fig. 6 The dependence of the FWHM and the integrated peak intensity of the PL spectrum as a function of excitation fluence.

interactions in its single crystals is a mechanism for emission enhancement. ASE from a large single crystal of BMSA was observed. The FWHM of the narrowed spectra reached 10 nm and the threshold of ASE was about 10 μJ pulse^{-1}. The observation of ASE with a low threshold value indicates that the BMSA crystals are good candidates for organic solid-state lasers.

We thank the National Basic Research Program of China (973 program, 2009CB623605) and the Program for New Century Excellent Talents in Universities of China Ministry of Education, the 111 Project (Grant no. B06009).

Experimental section

General remarks

All reagents and starting materials for the synthesis are commercially available and were used as received. THF and methyl-THF were purchased from Aldrich and used without further purification.

^{1}H NMR spectra were recorded at 298 K on an AVANCZ 500 spectrometer with tetramethylsilame (TMS) as the standard. Compounds were characterized by a Flash EA 1112, CHNS-O elemental analysis instrument. Time of flight mass spectra were recorded using a Kratos MALDI-TOF mass system.

UV-vis absorption spectra were recorded on a UV-3100 spectrophotometer. Fluorescence measurements were carried out with a RF-5301PC device. The fluorescence quantum yield (Φ_F) in solution was measured in dilute THF using quinine sulfate in 0.1 mol L^{-1} sulfuric acid as the standard. Crystalline state PL efficiencies were measured with an integrating sphere (C-701, Labsphere Inc.), using a 325 nm Xe light as the excitation source, and the laser was introduced into the sphere through the optical fiber. Low temperature measurements for samples were performed from a liquid nitrogen optical cryostat (Optistat DN-V). Time-resolved fluorescence measurements were performed on a time-correlated single photon counting (TCSPC) system. Fluorescence signals were collimated and focused onto the entrance slit of a monochromator with the output plane equipped with a photomultiplier tube (Hamamat-suH5783p), which was connected to a board (Becker & HickelSPC-130). A 405 nm picosecond diode laser (Edinburgh Instruments EPL-405, repetition rate 10 MHz) was used to excite the samples.

Single crystals of BMSA were prepared by vaporizing mixed solvents of chloroform and ethanol (2 : 1) slowly at room temperature under the rigorous exclusion of light. Diffraction experiments were carried out on a Rigaku R-AXIS RAPID diffractometer equipped with Mo-K_α radiation at 293(±2) K. The structures were solved by direct methods and refined by a full-matrix least-squares technique using the SHELXS v. 5.1 program.†

Synthesis of BMSA

A round-bottomed flask (25 mL) was oven dried and cooled under an N_2 atmosphere. 1-Methyl-4-vinylbenzene (0.28 g, 2.4 mmol), 9,10-dibromoanthracene (0.34 g, 1 mmol), K_3PO_4 (0.64 g, 3 mmol) and $Pd(OAc)_2$ were dissolved in dry DMAc (10 mL). The reaction mixture was heated to 110 °C in an oil bath and stirred for 24 h at this temperature. After being cooled to room temperature, the reaction mixture was poured into water and extracted with CH_2Cl_2 (3 × 40 mL). The combined organic extracts were washed with brine, dried (Mg_2SO_4) and concentrated to dryness under vacuum. The crude product was purified by flash column chromatography (petroleum ether/CH_2Cl_2 = 4 : 1) to give BMSA as a yellow solid (0.30 g, 73% yield). ^{1}H NMR (500 MHz $CDCl_3$) δ 2.43 (6H, s, CH_3), 6.91 (2H, d, J = 16.5 Hz, CH═CH), 7.27 (2H, d, J = 7.5 Hz, Ar), 7.45–7.47 (4H, m, Ar), 7.59 (2H, d, J = 8.0 Hz, Ar), 7.88 (2H, d, J = 16.5 Hz, CH═CH), 8.39–8.41 (4H, m, Ar); MALDI/TOF MS: Calc. for $C_{32}H_{36}$: 410.2. Found: 410.8. Anal. calc. for $C_{32}H_{26}$: C, 93.62; H, 6.38. Found: C, 93.56; H, 6.45.

Crystal data for BMSA

$C_{32}H_{26}$, M = 410.53, monoclinic, space group $P2_1/c$, a = 5.4103(11), b = 9.7287(19), c = 21.814(4) Å, α = 90.00, β = 94.84(3), γ = 90.00°, V = 1144.1(4) Å^3, T = 293(2) K, Z = 2, 10 691 reflections measured, 2592 independent reflections (R_{int} = 0.1441). The final R_1 values were 0.0990 ($I > 2\sigma(I)$). The final w$R(F^2)$ value was 0.1602 ($I > 2\sigma(I)$). The final R_1 value was 0.2362 (all data). The final w$R(F^2)$ value was 0.2073 (all data).†

Notes and references

1 (*a*) S. R. Forrest and E. T. Mark, *Chem. Rev.*, 2007, **107**, 923; (*b*) N. Tessler, G. J. Denton and R. H. Friend, *Nature*, 1996, **382**, 695; (*c*) F. Hide, M. B. Diaz-Garcia, J. Schwartz, M. Andersson, Q. Pei and A. J. Heeger, *Science*, 1996, **273**, 1833.

2 (*a*) R. H. Friend, R. W. Gymer, A. B. Holmes, J. H. Burroughes, R. N. Marks, C. Taliani, D. D. C. Bradley, D. A. Dos Santos, J. L. Bredas, M. Logdlund and W. R. Salaneck, *Nature*, 1999, **397**, 121; (*b*) J. Gierschner, M. Ehni, H.-J. Egelhaaf, B. Milián Medina, D. Beljonne, H. Benmansour and G. C. Bazan, *J. Chem. Phys.*, 2005, **123**, 144914; (*c*) K.-H. Schweikart, M. Hohloch, E. Steinhuber, M. Hanack, L. Lüer, J. Gierschner, H.-J. Egelhaaf and D. Oelkrug, *Synth. Met.*, 2001, **121**, 1641; (*d*) C. C. Wu, O. J. Korovyanko, M. C. DeLong, Z. V. Vardeny, J. J. Gutierrez and J. P. Ferraris, *Synth. Met.*, 2003, **139**, 735.

3 (*a*) D. Oelkrug, A. Tompert, J. Gierschner, H.-J. Egelhaaf, M. Hanack, M. Hohloch and E. Steinhuber, *J. Phys. Chem. B*, 1998, **102**, 1902; (*b*) J. Luo, Z. Xie, J. W. Y. Lam, C. H. Chen, C. Qiu, H. S. Kwok, X. Zhan, Y. Liu, D. Zhu and B. Z. Tang,

Chem. Commun., 2001, 1740; (*c*) Y. Hong, J. W. Y. Lam and B. Z. Tang, *Chem. Commun*., 2009, 4332.
4 (*a*) B.-K. An, S.-K. Kwon, S.-D. Jung and S. Y. Park, *J. Am. Chem. Soc*., 2002, **124**, 14410; (*b*) Z. Xie, B. Yang, F. Li, G. Cheng, L. Liu, G. Yang, H. Xu, L. Ye, M. Hanif, S. Liu, D. Ma and Y. Ma, *J. Am. Chem. Soc*., 2005, **127**, 14152; (*c*) Z. J. Ning, Z. Chen, Q. Zhang, Y. L. Yan, S. X. Qian, Y. Cao and H. Tian, *Adv. Funct. Mater*., 2007, **17**, 3799; (*d*) T. Zhou, F. Li, Y. Fan, W. Song, X. Mu, H. Zhang and Y. Wang, *Chem. Commun*., 2009, 3199.
5 (*a*) J. Chen, C. W. L. Charles, W. Y. L. Jacky, Y. Dong, M. F. L. Samuel, I. D. Williams, D. Zhu and B. Z. Tang, *Chem. Mater*., 2003, **15**, 1535; (*b*) Y. Ren, Y. Q. Dong, J. W. Y. Lam, B. Z. Tang and K. S. Wong, *Chem. Phys. Lett*., 2005, **402**, 468.
6 (*a*) N. Tessler, *Adv. Mater*., 1999, **11**, 363; (*b*) I. D. W. Samuel and G. A. Turnbull, *Chem. Rev*., 2007, **107**, 1272; (*c*) H. Yanagi, T. Ohara and T. Morikawa, *Adv. Mater*., 2001, **13**, 1452.
7 (*a*) M. Ichikawa, R. Hibino, M. Inoue, T. Haritani, S. Hotta, T. Koyama and Y. Taniguchi, *Adv. Mater*., 2003, **15**, 213; (*b*) M. Polo, A. Camposeo, S. Tavazzi, L. Raimondo, P. Spearman, A. Papagni, R. Cingolani and D. Pisignano, *Appl. Phys. Lett*., 2008, **92**, 083311; (*c*) Q. D. Chen, H. H. Fang, B. Xu, J. Yang, H. Xia, F. P. Chen, W. J. Tian and H. B. Sun, *Appl. Phys. Lett*., 2009, **94**, 201113.
8 (*a*) H. Xia, J. He, B. Xu, S. Wen, Y. Li and W. J. Tian, *Tetrahedron*, 2008, **64**, 5736; (*b*) J. He, B. Xu, F. Chen, H. Xia, K. Li, L. Ye and W. J. Tian, *J. Phys. Chem. C*, 2009, **113**, 9892; (*c*) B. Xu, H. Fang, F. Chen, H. Lu, J. He, Y. Li, Q. Chen, H. Sun and W. J. Tian, *New J. Chem*., 2009, **33**, 2457.
9 M. J. Frisch, G. W. Trucks, H. B. Schlegel, G. E. Scuseria, M. A. Robb, J. R. Cheeseman, J. A. Montgomery, Jr., T. Vreven, K. N. Kudin, J. C. Burant, J. M. Millam, S. S. Iyengar, J. Tomasi, V. Barone, B. Mennucci, M. Cossi, G. Scalmani, N. Rega, G. A. Petersson, H. Nakatsuji, M. Hada, M. Ehara, K. Toyota, R. Fukuda, J. Hasegawa, M. Ishida, T. Nakajima, Y. Honda, O. Kitao, H. Nakai, M. Klene, X. Li, J. E. Knox, H. P. Hratchian, J. B. Cross, V. Bakken, C. Adamo, J. Jaramillo, R. Gomperts, R. E. Stratmann, O. Yazyev, A. J. Austin, R. Cammi, C. Pomelli, J. Ochterski, P. Y. Ayala, K. Morokuma, G. A. Voth, P. Salvador, J. J. Dannenberg, V. G. Zakrzewski, S. Dapprich, A. D. Daniels, M. C. Strain, O. Farkas, D. K. Malick, A. D. Rabuck, K. Raghavachari, J. B. Foresman, J. V. Ortiz, Q. Cui, A. G. Baboul, S. Clifford, J. Cioslowski, B. B. Stefanov, G. Liu, A. Liashenko, P. Piskorz, I. Komaromi, R. L. Martin, D. J. Fox, T. Keith, M. A. Al-Laham, C. Y. Peng, A. Nanayakkara, M. Challacombe, P. M. W. Gill, B. G. Johnson, W. Chen, M. W. Wong, C. Gonzalez and J. A. Pople, *GAUSSIAN 03 (Revision A.01)*, Gaussian, Inc., Wallingford, CT, 2003.
10 H. C. Weiss, D. Blaser, R. Boese, B. M. Doughan and M. M. Haley, *Chem. Commun*., 1997, 1703.
11 (*a*) R. Taylor and O. Kennard, *J. Am. Chem. Soc*., 1982, **104**, 5063; (*b*) M. Nishio, *CrystEngComm*, 2004, **6**, 130.
12 W. B. Jennings, B. M. Farrell and J. F. Malone, *Acc. Chem. Res*., 2001, **34**, 885.
13 R. L. Christensen, A. Faksh, J. A. Meyers, I. D. W. Samuel, P. Wood, R. R. Schrock and K. C. Hultzsch, *J. Phys. Chem. A*, 2004, **108**, 8229.
14 C. J. Bhongale, C. W. Chang, C. S. Lee, E. W. G. Diau and C. S. Hsu, *J. Phys. Chem. B*, 2005, **109**, 13472.
15 N. Johansson, J. Salbeck, J. Bauer, F. Weissortel, P. Broms, A. Andersson and W. R. Salaneck, *Adv. Mater*., 1998, **10**, 1137.

